J. Phys. A: Math. Gen. 25 (1992) 4573–4594. Printed in the UK

Energy-level statistics of an integrable billiard system in a rectangle in the hyperbolic plane

Ch Grosche

International School for Advanced Studies, SISSA, Strada Costiera 11, 34014 Trieste, Miramare, Italy

Received 19 Feburary 1992

Abstract. A separable billiard system in the hyperbolic strip, a particular realization of the hyperbolic plane, is investigated. We consider a rectangle bounded by straight lines in the hyperbolic strip as an approximation of either a regular octagon with area $A = 4\pi$, or of a hyperbolic rectangle bounded by geodesics, respectively. Due to the simple geometry of our approximation the Schrödinger equation is separable, and leads to simple transcendental equations for the eigenvalues in terms of Legendre functions. The statistical properties of the eigenvalue spectrum are investigated and checked, with respect to Weyl's law, level spacing, number variance and spectral rigidity, respectively. In particular the numerical results for the spectral rigidity are in close agreement with the semi-classical theory of Berry.

1. Introduction

In recent years billiard systems have become increasingly popular. This is, of course, due to the accessibility of more powerful computers. Of special interest have been systems which allow the considerations of trace formulae. Let us consider a two-dimensional system. Take a test function $h(p) = h(-p)$, decreasing faster than $1/|p|^2$ for $|p| \to \infty$ and which is holomorphic in some appropriate strip $\mathrm{Im}(p)$. The motion of a classical particle in this two-dimensional system can described by its orbits. The trace of the propagator of the corresponding quantum system means that (in the sense of the semi-classical approximation) only the periodic orbits are relevant. Such trace formulae (Gutzwiller [1]) have provided powerful techniques in analysing the classical and quantum properties of chaotic billiard systems (see Friedrich and Wintgen [2], Sieber [3] and Sieber and Steiner [4] and references therein).

In the study of such billiard systems on Riemann surfaces, i.e. on compact polygons on the Poincaré upper half-plane $\mathcal{H}$ (Lobachevsky plane, hyperbolic plane) one is naturally led to the Selberg trace formula [5, 6] which is, however, an exact formula. Endowed with periodic boundary conditions these systems are highly chaotic (ergodic) and serve as an important example in the study of quantum chaos (quantum chaology [7]). Aurich *et al* [8, 9] have achieved for these particular systems a great deal of understanding, such that these systems can be understood as being numerically solved, including coming closer to an answer to the question 'Can one hear the shape of a drum?' [10, 11]. Another important billiard system is Artin's billiard, which has an application in the theory of the early universe [12]. Here similar results could be obtained [13].

0305-4470/92/174573+22$04.50

In this paper I want to study a particular approximation of a hyperbolic polygon in the hyperbolic strip (see figure 1). It is constructed as follows. Let us start with the Poincaré upper half-plane which is defined as

$$\mathcal{H} = \{\zeta = x + \mathrm{i}y | x \in \mathbf{R}, y > 0\} \tag{1.1}$$

endowed with the hyperbolic metric $\mathrm{d}s^2 = (\mathrm{d}^2x + \mathrm{d}^2y)/y^2$. By means of the Cayley transformation

$$\zeta = \frac{-\mathrm{i}z + \mathrm{i}}{z + 1} \qquad z = x_1 + \mathrm{i}x_2 = \frac{-\zeta + \mathrm{i}}{\zeta + \mathrm{i}} \tag{1.2}$$

the Poincaré upper half-plane is mapped onto the Poincaré disc with metric $g_{ab} = [2/(1 - r^2)]\,\mathrm{diag}(1, r^2)$ $(r^2 = x_1^2 + x_2^2)$, and by means of

$$\eta = X + \mathrm{i}Y = -\ln(-\mathrm{i}\zeta) = 2\tan^{-1} z \tag{1.3}$$

onto the hyperbolic strip with metric $g_{ab} = \delta_{ab}/\cos^2 Y$.

The study of classical and quantum motion in hyperbolic spaces emerges from three considerations.

(1) Hyperbolic spaces can serve as a model in cosmology [12, 14].
(2) Hyperbolic spaces play an important role in string theory [15], in particular in the mathematical theory of Riemann surfaces required in the multiloop expansion (D'Hoker and Phong [16]) in the Polyakov approach [17] to perturbation theory.
(3) Motion in hyperbolic space in (compact or non-compact) domains with periodic boundary conditions serves as an example for quantumchaos (Gutzwiller [18], Steiner [19]).

Usually the classical motion in a finite domain in hyperbolic geometry is chaotic. Consequently the quantum motion reflects some of the chaotic properties of the chaotic classical motion, e.g. there is in general level repulsion. However, are there simple models which are nevertheless separable and resemble some properties of hyperbolic space? Let us for example consider the motion in a bounded domain in a hyperbolic geometry where the boundaries are geodesics (with zero curvature). The everywhere negative curvature of hyperbolic space now causes that near lying geodesics to diverge exponentially in time evolution, i.e. they have a positive Lyapunov exponent. This means that the property of the space defocuses the classical trajectories (e.g. [20, 21]). However, if it is possible to choose boundaries which have a focusing property then it may be possible that the defocusing property of the hyperbolic space and the focusing property of the boundaries interact in such a way that the system remains separable and non-chaotic. The billiard system presented in this paper has exactly this property.

From the particular form our rectangle in the hyperbolic plane has, one could hope to gain some information about the (at least ground state) energy levels of the (classically chaotic) hyperbolic octagon with periodic boundary conditions. However, Aurich *et al* [8, 9] have actually solved the corresponding Schrödinger equation numerically for symmetric as well as asymmetric octagons [9] and therefore one can only compare results now and see if the integrable system resembles some properties of the chaotic one. Furthermore, there is a numerical study of hyperbolic triangles embedded in the regular octagon in the Poincaré disc with Dirichlet and Neumann

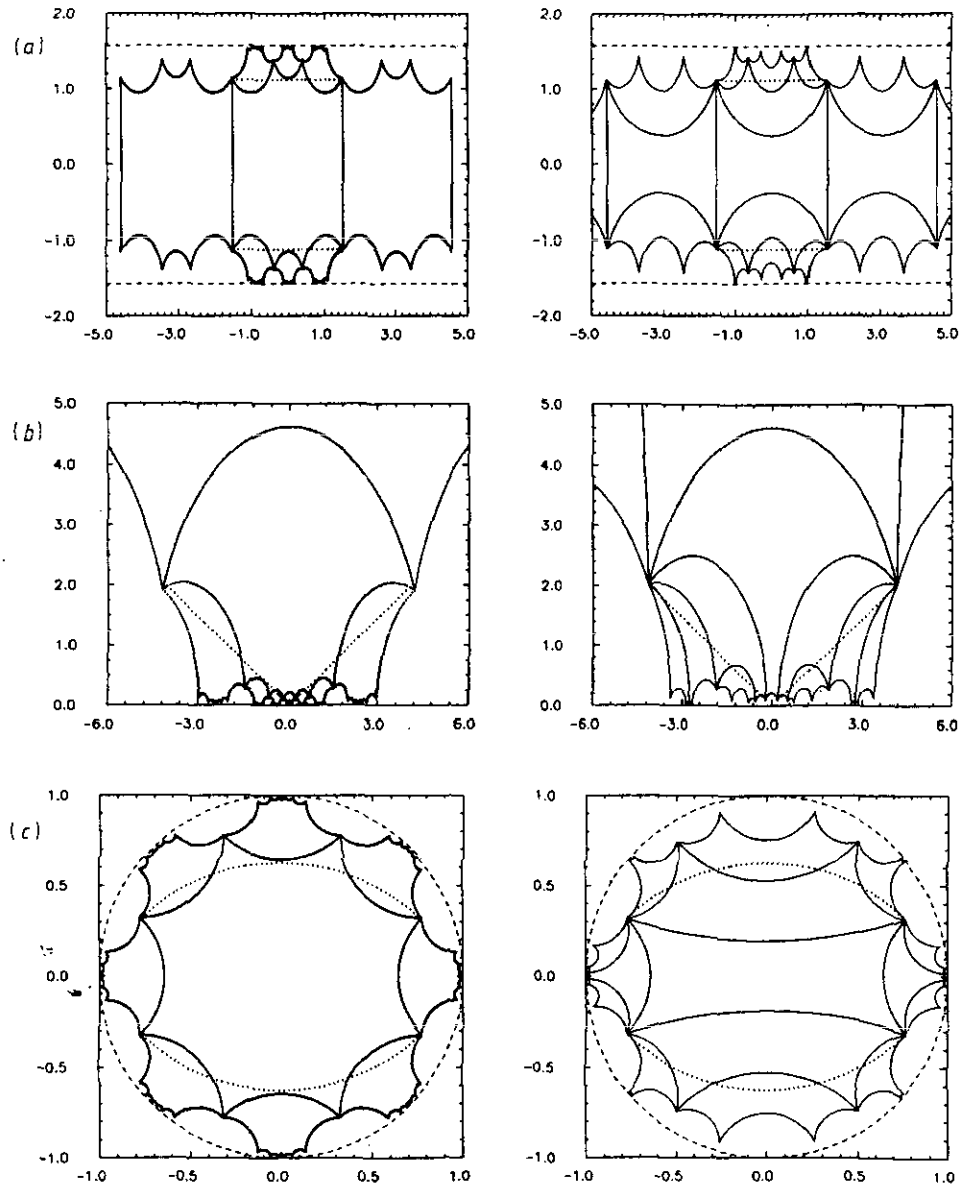

Figure 1. (*a*) Tesselations in the Hyperbolic Strip. (*b*) Tesselations in the Poincaré upper half-plane: The equivalent of (*a*) transformed onto $\mathcal{H}$. The boosts in the $\pm y$-direction for the octagon are hardly visible due to their enormous scaling. (*c*) Tesselations in the Poincaré disc: The equivalent of figure 1(*a*) transformed onto D.

boundary conditions, respectively, by Balazs *et al* [22, 23]. Nevertheless the idea remains to study billiards in unusual settings, e.g. the one presented here which serves as an example of a separable quantum billiard in hyperbolic geometry, see also Graham *et al* [24] for an integrable approximation of a cosmological billiard (Artin's billiard).

The further contents of this paper are now as follows: In section 2 I will describe

the 'rectangle approximation' in some detail and set up the quantization condition. Weyl's law for the various parity classes, respectively Dirichlet and Neumann boundary conditions, are formulated in order to check the increase of the number of energy levels with increasing energy.

Section 3 contains the numerical results and an investigation of the statistical properties of the calculated energy levels.

The forth section contains a discussion and a summary.

2. The system

Let us start with a description of the system which I call 'a rectangle in the hyperbolic plane'. In figures 1(*a*–*c*) I have displayed how the rectangle in the three realizations of the hyperbolic plane looks alike. In the hyperbolic strip it consists of two vertical straight lines which are geodesics (solid lines), and two horizontal straight lines which are not geodesics (dotted lines). In figures 1(*b*) and 1(*c*), respectively, it is also displayed how this rectangle looks like in the Poincaré upper half-plane and the Poincaré disc (dotted lines), respectively, and how the hyperbolic strip, the Poincaré upper half-plane and disc are tessalated by the symmetric octagon and hyperbolic rectangles (see below), respectively.

I also have displayed the regular octagon which corresponds to a Riemann surface of genus two, the simplest Riemann surface tesselating the hyperbolic plane. The regular octagon can be conveniently constructed in the Poincaré disc with eight quarter-circles described by [22]

$$\begin{pmatrix} x_1 \\ x_2 \end{pmatrix} = \begin{pmatrix} \tilde{r} - \hat{r}\cos\alpha \\ -\hat{r}\cos\alpha \end{pmatrix} \qquad -\tfrac{\pi}{4} \leqslant \alpha \leqslant \tfrac{\pi}{4} \qquad \tilde{r} = \sqrt{\tfrac{1}{2}(\sqrt{2}+1)} \qquad \hat{r} = \sqrt{\tfrac{1}{2}(\sqrt{2}-1)} \tag{2.1}$$

which give rise to the eight generators of the symmetric octagon in the Poincaré disc [8, 9, 22]

$$\gamma_k = \begin{pmatrix} \cosh\frac{L_0}{2} & \sinh\frac{L_0}{2}\mathrm{e}^{\mathrm{i}k\pi/4} \\ \sinh\frac{L_0}{2}\mathrm{e}^{-\mathrm{i}k\pi/4} & \cosh\frac{L_0}{2} \end{pmatrix} \qquad (k = 0,1,2,3) \tag{2.2}$$

including the inverse γ_k^{-1}, with $\cosh\frac{L_0}{2} = \cot\frac{\pi}{8} = 1+\sqrt{2} = 2.414\,213\,562\ldots$. L_0 is the length of the shortest closed periodic geodesic in the regular octagon [8]. From the geometry is it clear that the area of a rectangle in the hyperbolic strip is given by

$$A = \int_{X_a}^{X_b}\int_{Y_a}^{Y_b} \frac{\mathrm{d}X\mathrm{d}Y}{\cos^2 Y} = (X_b - X_a)(\tan Y_b - \tan Y_a) \tag{2.3}$$

with some numbers (X_a, X_b, Y_a, Y_b). Since the vertical lines coincide with the corresponding lines of the regular octagon, we choose as $-X_a = X_b = L_0/2$ with L_0 given by

$$L_0 = 2\ln\left(\frac{1+\sqrt{\sqrt{2}-1}}{1-\sqrt{\sqrt{2}-1}}\right) = 3.057\,141\,839\ldots. \tag{2.4}$$

From the definition of a rectangle $[-L_0/2, L_0/2] \times [-Y_0, Y_0]$ we have several possibilities in choosing a particular one. One can either choose for Y_0 the point Y_A given by the right upper corner of the octagon, the point Y_B given by the maximum value of the variable Y the octagon takes on in the strip, the point Y_C given by the minimum value of the variable Y the octagon takes on in the strip, or by some intermediate value Y_M given if the area of the rectangle equals, say $A = 4\pi$. Whereas the separability of the rectangle in the hyperbolic strip is obvious, the separability in the Poincaré upper half-plane and the Poincaré disc, respectively, is not so obvious. However, some particular polar coordinate systems (r, ϕ) do exist.

Explicitly these values are given by

$$\begin{aligned}
Y_A &= \tan^{-1}\left(\frac{\sqrt{2}}{\sqrt{\sqrt{2}-1}}\right) = 1.143\,717\,740\ldots \\
Y_B &= \tan^{-1}\left(\frac{\sqrt{\sqrt{2}+1}}{1-1/\sqrt{2}}\right) = 1.384\,478\,273\ldots \\
Y_C &= \tan^{-1}\left(\frac{\sqrt{\sqrt{2}+1}-\sqrt{\sqrt{2}-1}(\cos\omega-\sin\omega)}{1-\sqrt{2}+\cos\omega}\right) = 0.944\,946\,256\ldots \\
\omega &= \sin^{-1}\left(\frac{(\sqrt{2}-1)\sqrt{6-2\sqrt{2}}-2}{7-2\sqrt{2}}\right) = -0.307\,422\,594\ldots \\
Y_M &= \tan^{-1}\left(\frac{2\pi}{L_0}\right) = 1.117\,959\,030\ldots .
\end{aligned} \tag{2.5}$$

We have $Y_C < Y_M < Y_A < Y_B$. The two horizontal lines in figure 1(*a*) of the rectangle are not geodesics. It is nevertheless possible to construct a hyperbolic square bounded by geodesics. We consider the rectangle in the Poincaré upper half-plane and look for the arcs of a circle connecting the points $\zeta_A = e^{L_0/2}(\sin Y_0 + i\cos Y_0)$ and $\zeta_A' = e^{-L_0/2}(\sin Y_0 + i\cos Y_0)$. The circles described by $(x \mp x_r)^2 + y^2 = r^2$ with

$$x_r = \frac{\cosh\frac{L_0}{2}}{\sin Y_0} \qquad r = \sqrt{\frac{\cosh^2\frac{L_0}{2}}{\sin^2 Y_0} - 1} \tag{2.6}$$

do the job. The emerging domain in $\mathcal{H}$ can be seen as generated by the matrices

$$\begin{aligned}
\gamma_1 &= \begin{pmatrix} e^{L_0/2} & 0 \\ 0 & e^{-L_0/2} \end{pmatrix} \\
\gamma_2 &= \frac{1}{\sqrt{\cosh^2\frac{L_0}{2} - \sin^2 Y_0}} \begin{pmatrix} \cosh\frac{L_0}{2} & \sin Y_0 \\ \sin Y_0 & \cosh\frac{L_0}{2} \end{pmatrix}.
\end{aligned} \tag{2.7}$$

On the left-hand side in figures 1(*a–c*) I have displayed the action of applying the boosts of equation (2.2) to the fundamental domain of the regular octagon. Also shown is the 'rectangle approximation'. On the right the two-fold action of the generators of equation (2.7) is shown. Due to the general formula for a polygon in the hyperbolic plane $A = [(V-2)\pi - \sum\alpha]$, where V denotes the number

of vertices and α the corresponding angles (e.g. [22]), we get for the area of the hyperbolic square generated by the matrices (2.7)

$$\alpha = Y_0 + \tan^{-1}\left(\tan Y_0 - \frac{1+\mathrm{e}^{-L_0}}{\sin 2Y_0}\right)$$
$$A = 4\tan^{-1}\left(\frac{\mathrm{e}^{L_0}-1}{\sqrt{2\mathrm{e}^{L_0}(x_r^2+r^2)-\mathrm{e}^{2L_0}-1}}\right). \tag{2.8}$$

which gives $\alpha = 0.490\,923\,447\ldots$, $A = 4.319\,491\,516\ldots$ for $Y_0 = Y_M$ with the parameters $x_r = \pm 2.684\,818\,117\ldots$, $r = 2.491\,635\,672\ldots$, respectively. We can not expect that the ground state energy levels for the hyperbolic squares should be of comparable size with those of the square and the octagon due to the large difference in their geometry and area $\ll 4\pi$.

For reasons of practicability and simplicity we now make the choice

$$Y_0 = Y_M = \tan^{-1}\left(\frac{2\pi}{L_0}\right) \tag{2.9}$$

and denote by the notion 'rectangle in the hyperbolic plane' the rectangle in the strip bounded by the four straight lines as described above. This particular choice makes a reasonable compromise as to the total number of levels which can be calculated within the region of stability of the numerical investigation by a simple Fortran program. Also the width and length along the X- and Y-axis of this square are almost equal.

In order to set up our quantization conditions and Weyl's law we must discriminate between four parity classes in the hyperbolic rectangle and the lengths of its boundaries. The rectangle is symmetric with respect to the X- and Y-axis, hence we get the four classes $P_1 = (+,+)$, $P_2 = (+,-)$, $P_3 = (-,+)$ and $P_4 = (-,-)$.

Let us set up the quantization condition. The free wavefunctions in the entire strip are given by [25]

$$\Psi_{p,k}(X,Y) = \sqrt{\frac{p\sinh \pi p \cos Y}{4\pi^2(\cosh^2 \pi k + \sinh^2 \pi p)}}\,\mathrm{e}^{\mathrm{i}kX} P^{\mathrm{i}p}_{\mathrm{i}k-1/2}(\sin Y) \tag{2.10}$$

which are normalized solutions of the Schrödinger equation ($\hbar = 2m = 1$)

$$-\cos^2 Y(\partial_X^2 + \partial_Y^2)\Psi(X,Y) = E\Psi(X,Y). \tag{2.11}$$

The energy spectrum is $E = p^2 + \frac{1}{4}$ and I have used dimensionless units. Even and odd parity with respect to the X-coordinate yield the quantization condition with respect to the X-dependence

$$\text{even:} \qquad \cos\frac{L_0 k_l}{2} = 0 \to k_l = \frac{2\pi(l+\frac{1}{2})}{L_0} \qquad l = 0,1,2,\ldots \tag{2.12}$$

$$\text{odd:} \qquad \sin\frac{L_0 k_l}{2} = 0 \to k_l = \frac{2\pi l}{L_0} \qquad l = 1,2,3,\ldots. \tag{2.13}$$

Even and odd parity with respect to the Y-coordinate then give the quantization conditions

$$\text{even:} \qquad P^{\mathrm{i}p_n}_{\mathrm{i}k_l-1/2}(\sin Y_0) + P^{\mathrm{i}p_n}_{\mathrm{i}k_l-1/2}(-\sin Y_0) = 0 \tag{2.14}$$

$$\text{odd:} \qquad P^{\mathrm{i}p_n}_{\mathrm{i}k_l-1/2}(\sin Y_0) - P^{\mathrm{i}p_n}_{\mathrm{i}k_l-1/2}(-\sin Y_0) = 0.. \tag{2.15}$$

The last two equations are transcendental equations for p_n, $n = 1, 2, \ldots$ and must be solved numerically. Actually one uses the representation

$$P^{ip}_{ik-1/2}(\sin Y) = \frac{1}{\Gamma(1-ip)}\left(\frac{1+\sin Y}{1-\sin Y}\right)^{ip/2} \times {}_2F_1\left(\frac{1}{2}-ik, \frac{1}{2}+ik; 1-ip; \frac{1-\sin Y}{2}\right) \tag{2.16}$$

and omits the $1/\Gamma(1-ip)$-factor. The energy of the nth level finally has the form

$$E_n = p_n^2 + \tfrac{1}{4}. \tag{2.17}$$

Let us first concentrate on the $(-,-)$ case, the others are similar, of course. We have $A = \pi$ for $Y_0 = Y_M$ in all parity classes. Weyl's law [26] describes the mean of the number of energy levels up to a certain energy, i.e. $\bar{N}(E) = \{\#N(\text{levels with energy } E) \quad E < E_N\}$. According to Baltes and Hilf [27] and Stewartson and Waechter [28] (for earlier results and generalizations see Baltes [29], Brownell [30], Kac [11] and Waechter [31]) one obtains for a two dimensional quantum system with Dirichlet boundary conditions on all boundaries (e.g. following [23, 24])

$$\bar{N}(E) = \frac{A}{4\pi}E - \frac{\partial A}{4\pi}\sqrt{E} + \frac{1}{24}\sum_{\text{corners}}\left(\frac{\pi}{\alpha_r} - \frac{\alpha_r}{\pi}\right) + \frac{1}{12\pi}\iint_A K(\sigma)\,\mathrm{d}^2\sigma - \frac{1}{24\pi}\oint_{\partial A}\kappa(s)\,\mathrm{d}s + \mathrm{O}\left(\frac{1}{\sqrt{E}}\right). \tag{2.18}$$

Here α_r denotes the angle of the rth corner, A the area of the system and ∂A the length of its boundary. Here K is the Gaussian curvature (here $K = -1$), $\mathrm{d}^2\sigma$ the surface integral, and the boundary mean curvature κ is given by

$$\kappa(s) = -2t^a(s)g_{ab}(s)\frac{\mathrm{D}}{\mathrm{D}s}n^b(s). \tag{2.19}$$

$n(s), t(s)$ is the normal (tangential) vector along the boundary, and the covariant derivative $\mathrm{D}/\mathrm{D}s$ is given by

$$\frac{\mathrm{D}}{\mathrm{D}s}n^a(s) = \frac{\mathrm{d}}{\mathrm{d}s}\frac{\mathrm{d}n^a}{\mathrm{d}s} + \Gamma^a_{bc}(s)\frac{\mathrm{d}t^b}{\mathrm{d}s}\frac{\mathrm{d}n^c}{\mathrm{d}s}, \tag{2.20}$$

Γ^a_{bc} is the Christoffel symbol. In the case where one considers the shifted Laplacian $-\Delta - 1/4$ the E-independent terms in $\bar{N}(E)$ change into [23]

$$c_0 = \frac{1}{24}\sum_{\text{corners}}\left(\frac{\pi}{\alpha_r} - \frac{\alpha_r}{\pi}\right) + \frac{1}{48\pi}\iint_A K(\sigma)\,\mathrm{d}^2\sigma - \frac{1}{96\pi}\oint_{\partial A}\kappa(s)\,\mathrm{d}s \tag{2.21}$$

This suffices for our purposes. Using the general formula for the length of a curve in a curved space

$$s = \int_{t_i}^{t_f}\sqrt{g_{11}\dot{x}^2 + g_{22}\dot{y}^2 + g_{12}\dot{x}\dot{y}}\,\mathrm{d}t \tag{2.22}$$

we obtain for the length of the boundary of a quarter rectangle

$$\partial A = 2\ln\left(\frac{1+\sin Y_0}{\cos Y_0}\right) + \frac{L_0}{2}\left(1+\frac{1}{\cos Y_0}\right). \tag{2.23}$$

Note that the vertical lines are geodesics and therefore their length can also be evaluated by the two-point formula in the strip

$$\cosh d(q'',q') = \frac{\cosh(X''-X')}{\cos Y' \cos Y''} - \tan Y' \tan Y''. \tag{2.24}$$

We have $\alpha_r = \pi/2$ $(r = 1,2,3,4)$ and therefore for the (X,Y) (odd, odd) states

$$\bar{N}(E)^{(-,-)} \simeq \frac{L_0 \tan Y_0}{8\pi} E - \frac{\sqrt{E}}{4\pi}\left[2\ln\left(\frac{1+\sin Y_0}{\cos Y_0}\right) + \frac{L_0}{2}\left(1+\frac{1}{\cos Y_0}\right)\right] + \frac{1}{4} - \frac{1}{48} + \frac{L_0 \tan Y_0}{192\cos^2 Y_0} \tag{2.25}$$

where we have allowed some arbitrary Y_0. Similarly for (X,Y) (odd, even) states

$$\bar{N}(E)^{(-,+)} \simeq \frac{L_0 \tan Y_0}{8\pi} E - \frac{\sqrt{E}}{4\pi}\left[2\ln\left(\frac{1+\sin Y_0}{\cos Y_0}\right) + \frac{L_0}{2}\left(\frac{1}{\cos Y_0}-1\right)\right] - \frac{1}{48} + \frac{L_0 \tan Y_0}{192\cos^2 Y_0}. \tag{2.26}$$

For (X,Y) (even, odd) states

$$\bar{N}(E)^{(+,-)} \simeq \frac{L_0 \tan Y_0}{8\pi} E - \frac{L_0}{8\pi}\left(\frac{1}{\cos Y_0}+1\right)\sqrt{E} - \frac{1}{48} + \frac{L_0 \tan Y_0}{192\cos^2 Y_0}. \tag{2.27}$$

For (X,Y) (even, even) states

$$\bar{N}(E)^{(+,+)} \simeq \frac{L_0 \tan Y_0}{8\pi} E - \frac{L_0}{8\pi}\left(\frac{1}{\cos Y_0}-1\right)\sqrt{E} - \frac{1}{48} + \frac{L_0 \tan Y_0}{192\cos^2 Y_0}. \tag{2.28}$$

For the entire square, of course, we have

$$\bar{N}(E) \simeq \frac{L_0 \tan Y_0}{2\pi} E - \frac{\sqrt{E}}{4\pi}\left[4\ln\left(\frac{1+\sin Y_0}{\cos Y_0}\right) + \frac{2L_0}{\cos Y_0}\right] + \frac{1}{4} - \frac{1}{12} + \frac{L_0 \tan Y_0}{48\cos^2 Y_0}. \tag{2.29}$$

Hence the odd parities in X and Y, respectively, give Dirichlet boundary conditions on the lines $Y = 0$ and $X = 0$, respectively, and even parities X and Y, respectively, give Neumann boundary conditions on the lines $Y = 0$ and $X = 0$, respectively. Of course, the Schrödinger equation restricted to our particular rectangle is not invariant with respect to translations in the Y-direction (it is in the X-direction). The Schrödinger operator is only invariant with respect to elements of a Fuchsian group, i.e. generators of hyperbolic polygons tesselating the hyperbolic plane.

3. Numerical results

The following table shows the first 25 levels for the parity classes $(-,-)$, $(-,+)$, $(+,-)$ and $(+,+)$, respectively. The last figure may be uncertain. The energy levels are ordered according to increasing energy, of course, and in addition I also display the corresponding quantum number-pairing (l,n) arising from the X- and Y-quantization condition of the transcendental equations for p_n, respectively.

A more comprehensive list of energy levels shows that we have level clustering (degeneracies or almost degeneracies) which are expected for separable systems (compare the short enumeration in table 2). There is also an asymptotic behaviour of the Legendre functions which give for $p \to \infty$ and fixed k_l the solution of equations (2.14) and (2.15) (independent of k_l)

$$p_n = 2\pi n \left[\ln\left(\frac{1+\sin Y_0}{1-\sin Y_0}\right)\right]^{-1} = 2.139\,942\,066\ldots \qquad (n \in \mathbf{N},\ p_n \to \infty) \quad (3.1)$$

which is nicely confirmed by the data.

Table 1. The first 25 levels $E_N^{(-,-)}$, $E_N^{(-,+)}$ $E_N^{(+,-)}$ and $E_N^{(+,+)}$

$E_N^{(-,-)}(l,n)$	$E_N^{(-,+)}(l,n)$	$E_N^{(+,-)}(l,n)$	$E_N^{(+,+)}(l,n)$
$E_1 = 7.5219(1,1)$	$E_1 = 4.8994(1,1)$	$E_1 = 5.6255(0,1)$	$E_1 = 2.4360(0,1)$
$E_2 = 14.638(2,1)$	$E_2 = 13.368(1,2)$	$E_2 = 10.575(1,1)$	$E_2 = 8.7781(1,1)$
$E_3 = 21.340(1,2)$	$E_3 = 13.672(2,1)$	$E_3 = 19.373(0,2)$	$E_3 = 11.365(0,2)$
$E_4 = 25.131(3,1)$	$E_4 = 22.071(2,2)$	$E_4 = 19.539(2,1)$	$E_4 = 16.848(1,2)$
$E_5 = 29.366(2,2)$	$E_5 = 24.992(3,1)$	$E_5 = 24.656(1,2)$	$E_5 = 19.136(2,1)$
$E_6 = 38.038(4,1)$	$E_6 = 31.633(1,3)$	$E_6 = 31.315(3,1)$	$E_6 = 29.283(2,2)$
$E_7 = 42.999(3,2)$	$E_7 = 38.026(4,1)$	$E_7 = 35.493(2,2)$	$E_7 = 29.675(0,3)$
$E_8 = 44.220(1,3)$	$E_8 = 38.366(3,2)$	$E_8 = 42.267(0,4)$	$E_8 = 31.272(3,1)$
$E_9 = 52.118(2,3)$	$E_9 = 39.596(2,3)$	$E_9 = 45.277(4,1)$	$E_9 = 34.925(1,3)$
$E_{10} = 53.020(5,1)$	$E_{10} = 53.019(3,3)$	$E_{10} = 47.493(1,3)$	$E_{10} = 45.274(4,1)$
$E_{11} = 61.589(4,2)$	$E_{11} = 53.445(5,1)$	$E_{11} = 51.760(3,2)$	$E_{11} = 45.723(2,3)$
$E_{12} = 65.593(3,3)$	$E_{12} = 59.099(1,4)$	$E_{12} = 58.134(2,3)$	$E_{12} = 48.841(3,2)$
$E_{13} = 70.000(6,1)$	$E_{13} = 60.084(4,2)$	$E_{13} = 61.261(5,1)$	$E_{13} = 57.149(0,4)$
$E_{14} = 76.269(1,4)$	$E_{14} = 66.961(2,4)$	$E_{14} = 72.287(4,2)$	$E_{14} = 61.261(5,1)$
$E_{15} = 83.689(5,2)$	$E_{15} = 69.996(6,1)$	$E_{15} = 74.321(0,4)$	$E_{15} = 62.362(1,4)$
$E_{16} = 84.107(2,4)$	$E_{16} = 74.736(4,3)$	$E_{16} = 74.552(3,3)$	$E_{16} = 63.008(3,3)$
$E_{17} = 85.049(4,3)$	$E_{17} = 80.296(3,4)$	$E_{17} = 79.220(6,1)$	$E_{17} = 71.645(4,2)$
$E_{18} = 88.931(7,1)$	$E_{18} = 83.451(5,2)$	$E_{18} = 79.525(1,4)$	$E_{18} = 72.926(2,4)$
$E_{19} = 97.349(3,4)$	$E_{19} = 88.931(7,1)$	$E_{19} = 90.038(2,4)$	$E_{19} = 79.220(6,1)$
$E_{20} = 108.24(6,2)$	$E_{20} = 95.729(1,5)$	$E_{20} = 95.691(5,2)$	$E_{20} = 88.740(4,3)$
$E_{21} = 109.80(8,1)$	$E_{21} = 99.500(4,4)$	$E_{21} = 97.078(4,3)$	$E_{21} = 89.131(3,4)$
$E_{22} = 110.55(5,3)$	$E_{22} = 103.55(2,5)$	$E_{22} = 99.126(7,1)$	$E_{22} = 93.783(0,5)$
$E_{23} = 116.27(4,4)$	$E_{23} = 104.65(5,3)$	$E_{23} = 106.08(3,4)$	$E_{23} = 95.610(5,2)$
$E_{24} = 117.48(1,5)$	$E_{24} = 108.22(6,2)$	$E_{24} = 115.54(0,5)$	$E_{24} = 98.981(1,5)$
$E_{25} = 125.29(2,5)$	$E_{25} = 109.80(8,1)$	$E_{25} = 120.73(1,5)$	$E_{25} = 99.126(7,1)$

For $E_{\max} \leqslant 1000$ we have $\#N^{(-,-)} = 229$, $\#N^{(-,+)} = 237$, $\#N^{(+,-)} = 240$, $\#N^{(+,+)} = 246$. The ground states for the four parity classes are $E_0^{(+,+)} = 2.4360$, $E_0^{(-,+)} = 4.8994$, $E_0^{(+,-)} = 5.6255$ and $E_0^{(-,-)} = 7.5219$, respectively, with $E_0^{(+,+)}$ as the lowest lying level.

Note the proximity of the lowest three eigenvalues to the lowest two eigenvalues $E_0^{\mathrm{oct}} = 3.8388$, $E_1^{\mathrm{oct}} = 5.353$ of the regular octagon [8] (which are however threefold and fourfold degenerate, respectively). The additional corners in the hyperbolic plane of the regular octagon hence do not increase the value of its ground state too significantly which is due to $A^{\mathrm{oct}} = 4\pi$.

The check with Weyl's law confirms the data nicely down to the lowest eigenvalues. The staircase (or step function) $N(E)$ (solid line) and Weyl's law (dotted line) are hardly distinguishable. See figure 9 for an enlargement. Let us consider

$$\delta_n = \#(\text{levels}) - \bar{N}(E) - 0.5. \tag{3.2}$$

The accumulated mean values of $\bar{\delta}$ (solid line) are consistent with zero, with fluctuations $|\bar{\delta}| = \mathrm{O}(10^{-2})$ about zero as shown in figure 4. Note the large fluctuations δ_n (dotted lines) of the actual step function about the mean value described by Weyl's law. This feature of large fluctuations is well known in integrable systems. Chaotic systems are typically smoother.

In figure 2 I have displayed for all four parity classes the step function and the corresponding Weyl's law, respectively.

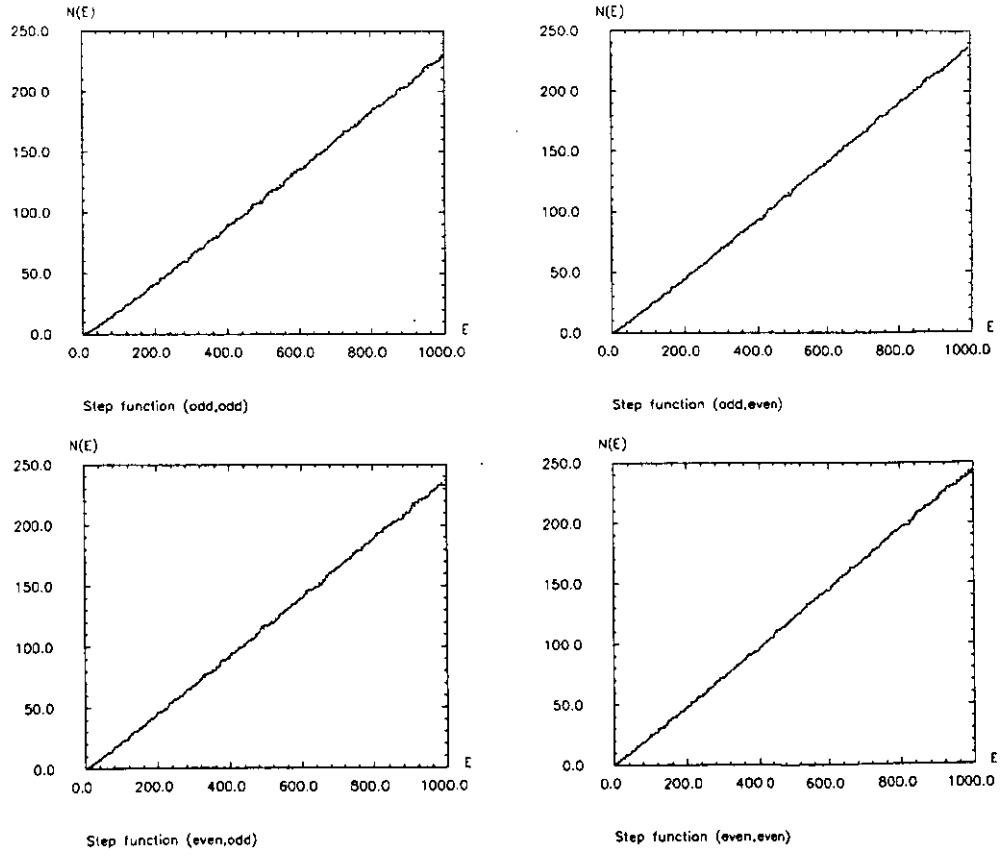

Figure 2. Step-function and Weyl's law of the calculated energy values for the four parity classes, i.e $E^{(-,-)}$, $E^{(-,+)}$ (top), $E^{(+,-)}$ and $E^{(+,+)}$ (bottom).

Table 2. Some almost degenerate energy levels

$E_N^{(-,-)}(l,n)$	$E_N^{(-,+)}(l,n)$	$E_N^{(+,-)}(l,n)$	$E_N^{(+,+)}(l,n)$
$E_{29} \approx 141.10(6,3)$	$E_{84} = 366.57(8,7)$	$E_{60} = 269.68(9,3)$	$E_{34} = 144.68(9,1)$
$E_{30} \approx 141.25(5,4)$	$E_{85} = 366.62(9,6)$	$E_{61} = 269.87(7,5)$	$E_{35} = 144.77(1,6)$
$E_{65} \approx 299.14(9,4)$	$E_{36} = 160.00(5,5)$	$E_{82} = 363.00(8,6)$	$E_{60} = 252.58(6,6)$
$E_{66} \approx 299.19(12,2)$	$E_{37} = 160.11(7,4)$	$E_{83} = 363.15(16,1)$	$E_{61} = 252.60(7,5)$
$E_{92} \approx 421.21(15,2)$	$E_{96} = 421.21(15,2)$	$E_{136} = 586.29(3,11)$	$E_{88} = 363.11(3,9)$
$E_{93} \approx 421.32(18,1)$	$E_{97} = 421.32(18,1)$	$E_{137} = 586.37(18,2)$	$E_{89} = 363.15(16,1)$
$E_{131} \approx 577.84(3,11)$	$E_{118} = 507.87(1,11)$		$E_{140} = 573.33(11,7)$
$E_{132} \approx 577.93(13,5)$	$E_{119} = 507.88(6,10)$		$E_{141} = 573.37(21,1)$
$E_{133} \approx 586.72(7,10)$	$E_{121} = 515.93(2,11)$		$E_{174} = 716.31(6,12)$
$E_{134} \approx 586.84(9,9)$	$E_{122} = 515.99(12,5)$		$E_{175} = 716.35(18,3)$

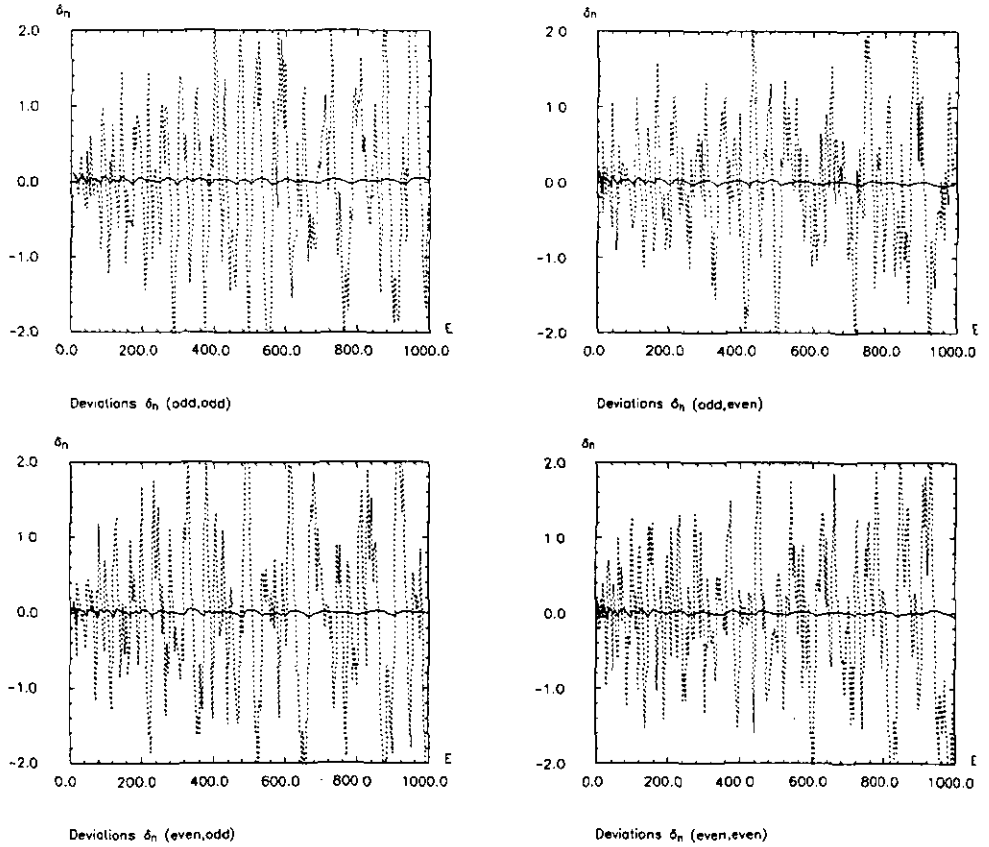

Figure 3. Deviations δ_n from Weyl's law for the four parity classes, i.e $E^{(-,-)}$, $E^{(-,+)}$ (top), $E^{(+,-)}$ and $E^{(+,+)}$ (bottom).

A first analysis now gives the level-spacing distribution $P(S)$ of spacing between neighbouring levels. Classically integrable systems belong to the universality class of uncorrelated level sequences. $P(S)$ is calculated for the scaled energy spectrum, which has a mean level spacing of one ($\approx \hbar$). One applies Weyl's law onto the

calculated energy levels and obtains the normalized levels E'_n by

$$E'_n = N(E_n) \tag{3.3}$$

and quantities for the scaled spectrum are denoted by a prime in the following. In integrable systems one typically has level clustering, which is expressed by $P(S) \to 1$ as $S \to 0$, whereas chaotic systems show level repulsion, i.e. $P(S) \to 0$ as $S \to 0$. The functional form of the nearest neighbour level spacing $P(S)$ for classically integrable systems has the form

$$P(S) = \mathrm{e}^{-S} \tag{3.4}$$

which is a Poisson distribution, whereas the result from random matrix theory for the level spacing distribution of a GOE ensemble is approximated by a Wigner distribution

$$P(S) = \frac{\pi}{2} S \mathrm{e}^{-\pi S^2/4} \tag{3.5}$$

and the corresponding level spacing distribution of a GUE-ensemble is given by

$$P(S) = \frac{32}{\pi^2} S^2 \mathrm{e}^{-4S^2/\pi}. \tag{3.6}$$

Figure 4 shows the analysis of our system and the consistence with a Poisson distribution (dotted line) is evident. The corresponding level spacing distributions for GUE (Gaussian unitarian ensemble) is denoted by the dashed line, and for GOE (Gaussian orthogonal ensemble) by the dashed-dotted line. Clearly GUE and GOE distributions are excluded.

A similar feature was first observed by Casati *et al* [32] for the flat rectangular billiard. With the chosen ΔS, the actual level distribution shows nevertheless fluctuations about the Poisson distribution. Making ΔS smaller would increase these fluctuations. The calculated χ^2-test gives values for $\Delta S = 0.2$ (0.1) $\chi^2 = 30.8$ (57.2) (odd, odd), $\chi^2 = 36.6$ (56.0) (odd, even), $\chi^2 = 19.6$ (47.5) (even, odd), and $\chi^2 = 28.1$ (54.1) (even, even), respectively, which gives confidence levels $\alpha = 0.17$ (0.23) (odd, odd), $\alpha = 0.05$ (0.26) (odd, even), $\alpha = 0.71$ (0.57) (even, odd), and $\alpha = 0.26$ (0.33) (even, even), respectively. This shows that the actual distribution is reasonable Poisson. Note the difference to e.g. [32] where in spite of the fact that there were some 100 times as many energy levels taken into account, the emerging level statistics had negligible confidence level.

We can also study the integrated level spacing

$$I(S) = \int_0^S P(t)\,\mathrm{d}t \tag{3.7}$$

which yields a useful statistics even for a small sample of level spacings. This gives

$$I_{\mathrm{Poisson}}(S) = 1 - \mathrm{e}^{-S} \qquad I_{\mathrm{GOE}}(S) = 1 - \mathrm{e}^{-\pi S^2/4} \tag{3.8}$$

and a non-analytical expression for $I_{\mathrm{GUE}}(S)$. Figure 5 shows good confirmation of the data with Poisson distributed energy levels.

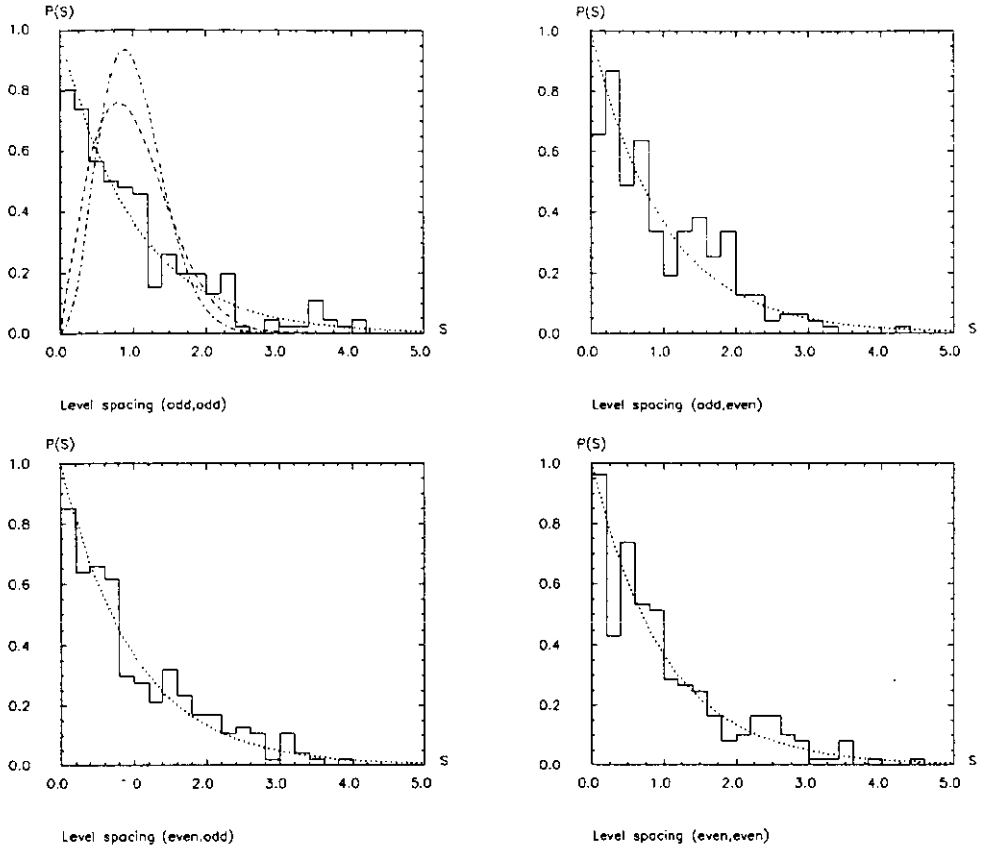

Figure 4. Nearest level spacing distribution $P(S)$ for the four parity classes, i.e $E^{(-,-)}$, $E^{(-,+)}$ (top), $E^{(+,-)}$ and $E^{(+,+)}$ (bottom).

The level spacing distribution $P(S)$ is a short range statistics. Another important tool in the analysis of the spectrum is the number variance $\Sigma^2(L)$ and the spectral rigidity $\Delta_3(L)$ [33], respectively. $\Sigma^2(L)$ is defined as the local variance of the number $n(E', L)$ of scaled energy levels in the interval from $E' - L/2$ to $E' + L/2$. It has the form

$$\Sigma^2(L) = \langle n(E', L) - L^2 \rangle . \tag{3.9}$$

The Δ_3 statistics of Metha and Dyson [33] is defined as the local average of the mean square deviation of the staircase from the best fitting of a straight line over an energy range corresponding to L mean level spacings, namely

$$\Delta_3(L) = \left\langle \min_{(a,b)} \frac{1}{L} \int_{-L/2}^{L/2} \mathrm{d}\epsilon \left[N'(E' + \epsilon) - a - b\epsilon \right]^2 \right\rangle . \tag{3.10}$$

It can be expressed as

$$\Delta_3(L) = \left\langle \frac{1}{L} \int_{-L/2}^{L/2} \mathrm{d}\epsilon N'^2(E' + \epsilon) - \left[\frac{1}{L} \int_{-L/2}^{L/2} \mathrm{d}\epsilon N'(E' + \epsilon) \right]^2 - 12 \left[\frac{1}{L^2} \int_{-L/2}^{L/2} \mathrm{d}\epsilon N'(E' + \epsilon) \right]^2 \right\rangle . \tag{3.11}$$

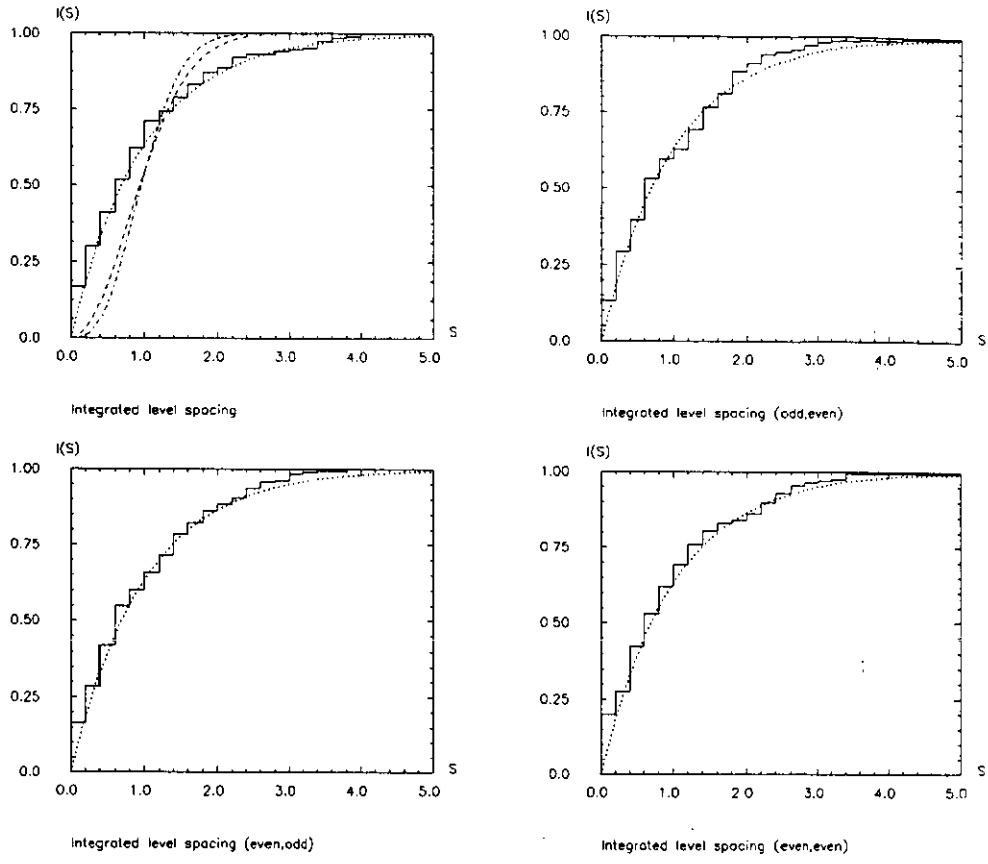

Figure 5. Integrated level spacing distribution $I(S)$ for the four parity classes, i.e $E^{(-,-)}$, $E^{(-,+)}$ (top), $E^{(+,-)}$ and $E^{(+,+)}$ (bottom).

As the number variance, it characterizes long-term correlations of the energy levels. Both statistics are related by

$$\Delta_3(L) = \frac{2}{L_4}\int_0^L \mathrm{d}s(L^3 - 2L^2 s - s^3)\Sigma^2(s). \tag{3.12}$$

Whenever $L \ll 1$, the very fact that $N(E)$ is a staircase leads in this limit to [35]

$$\Sigma^2(S) = L \qquad \Delta_3(L) = L/15 \tag{3.13}$$

and both statistics are linear and show the so-called Poisson behaviour, i.e. in the case of a genuine Poisson distributed level sequence, these results are exact.

The spectral rigidity gives, therefore, no information about the very finest scales corresponding to the spacings between neighbouring levels, whether they are Poisson distributed or not. Its usefulness lies in the way it describes level sequences larger than the inner energy scale ($L = 1$) of a system. Berry [35] has developed a semi-classical theory of the spectral rigidity and has shown that one must discriminate between at least three universality classes of rigidity, depending on whether one deals with classically integrable systems or classically chaotic systems. The first universality

class occurs for classically integrable systems. Here the Poisson $L/15$-form for the spectral rigidity extends from $L = 0$ to L_{max}. L_{max} corresponds to an outer energy scale $\propto 1/T_{min}$ (the inner energy scale corresponds to $L \simeq 1$), where T_{min} is the period of the shortest classical orbit and $L_{max} \propto \hbar^{N-1}$, and $\propto 1/\hbar$ for $N = 2$ (i.e. a two-dimensional system). The properties of the rigidity are determined by the contributions of the very short orbits. These orbits have a non-universal behaviour, which differ from system to system. As a consequence of the fact that there is a shortest orbit, the spectral rigidity saturates and approaches a non-universal constant Δ_∞ as $L \to \infty$ (and the same line of reasoning is true for the number variance Σ^2) [3, 9, 35].

The number variance for a GOE distributed sequences is given by [33, 34, 36]

$$\Sigma^2(L) = \frac{2}{\pi^2}\left\{ \log(2\pi L) + \gamma + 1 + \frac{1}{2}\,\mathrm{Si}^2(\pi L) - \frac{\pi}{2}\,\mathrm{Si}(\pi L) - \cos(2\pi L) - \mathrm{Ci}(2\pi L) + \pi^2 L\left[1 - \frac{2}{\pi}\,\mathrm{Si}(2\pi L)\right]\right\} \tag{3.14}$$

and for GUE-distributed sequences [3, 9, 34, 36], respectively,

$$\Sigma^2(L) = \frac{1}{\pi^2}\left\{ \log(2\pi L) + \gamma + 1 - \cos(2\pi L) - \mathrm{Ci}(2\pi L) + \pi^2 L\left[1 - \frac{2}{\pi}\,\mathrm{Si}(2\pi L)\right]\right\}. \tag{3.15}$$

Results for the spectral rigidity are obtained via the relation (3.13).

Let us consider the entire square in the hyperbolic plane. First of all, we see that all predicted features in fact occur. The χ^2-test however gives for $P(S)$, $\chi^2 = 77.9$, $\chi^2 = 118$ and $\chi^2 = 290$ for $\Delta S = 0.25, 0.20$ and 0.10, respectively, with confidence levels of $\alpha = O(10^{-7})$ and smaller, with respect to a Poisson distributed sequence which is negligible. Let us note that the superposition statistics according to [37] gives no improvement in the confidence level.

The number variance and spectral rigidity approach their L- and $L/15$-behaviour, respectively, for $L \to 0$. For L large, the number variance starts oscillating about a mean value and the spectral rigidity approaches a saturation value. This is true for all symmetry classes and for the analysis of the entire square as well.

We can explain our results in terms of the periodic orbit theory of Berry [35]. Of course, L_0 is the length on a closed periodic orbit which corresponds to motion along the X-axis. L_1 with $L_1 = 2\ln[(1 + \sin Y_0)/(\cos Y_0)] = 2.936\,147\,388\ldots$ is the length of an orbit along the Y-axis and is slightly shorter than the former one. However, these two shortest closed orbits are almost equal such that we can apply Berry's theory of the spectral rigidity in its simplest way.

For a classically integrable system the spectral rigidity approaches for $L > L_{max}$ a value Δ_∞ which is given by $\Delta_\infty = \text{constant} \times \sqrt{\mathcal{E}}$, where $\mathcal{E}$ denotes the scaled energy range over which the spectral rigidity has been evaluated. In the case of a flat square with sides $a = b = 1$, Δ_∞ can be evaluated as

$$\Delta_\infty \simeq \pi^{-5/2}\left[\zeta\left(\tfrac{3}{2}\right)\beta\left(\tfrac{3}{2}\right) - \tfrac{1}{2}\zeta(3)\right]\sqrt{\mathcal{E}} \simeq 0.0947\sqrt{\mathcal{E}}. \tag{3.16}$$

Similarly, $L_{max} \simeq \sqrt{\pi\mathcal{E}}$. According to e.g. [3, 9] this gives a prediction for the number variance $\Sigma^2(L)$ for $L > L_{max}$, i.e. $\Sigma_\infty = 2\Delta_\infty + O(1/L^3)$ (fluctuations

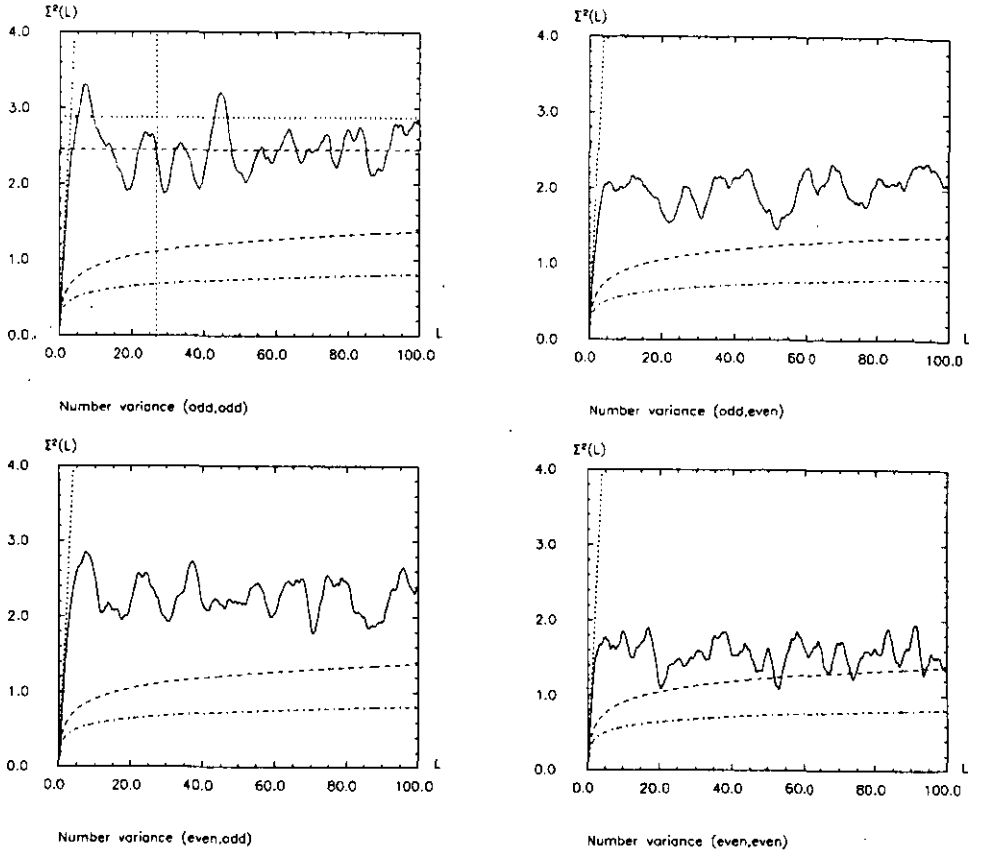

Figure 6. Number variance $\Sigma^2(L)$ for the four parity classes, i.e $E^{(-,-)}$, $E^{(-,+)}$ (top), $E^{(+,-)}$ and $E^{(+,+)}$ (bottom).

neglected, this behaviour explains why Σ^2 saturates much faster than Δ_3, see below). Assuming now that our square can be further approximated by a flat square with sides $a = L_0 \simeq b = L_1$, we obtain the following quantities for the (odd, odd) eigenstates of the square in the hyperbolic plane with $\#N = 229$ calculated energy values (Δ_∞, Σ_∞ are lower bounds)

$$L_{\max} \simeq 27 \qquad \Sigma_\infty^{\text{theory}} \simeq 2.874 \qquad \Delta_\infty^{\text{theory}} \simeq 1.437. \tag{3.17}$$

The numerical results are

$$\Sigma_\infty^{\text{num}} \simeq 2.454 \qquad \Delta_\infty^{\text{num}} \simeq 1.182. \tag{3.18}$$

with $\Sigma_\infty^{\text{num}} - 2\Delta_\infty^{\text{num}} \simeq 0.09$. Here $\Sigma_\infty^{\text{num}}$ is determined by taking the mean value of $\Sigma(L)$ above $L = 10$. In order to determine $\Delta_\infty^{\text{num}}$, a fit of the numerical result with the ansatz

$$\Delta_3(L) = \Delta_\infty\left(1 - \frac{a}{L} - \frac{b}{L^2}\right) \qquad L > L_{\max} \tag{3.19}$$

is made with $a = 0.0002081$ and $b = 43.90$, respectively. In figures 6 and 7, I have indicated the theoretical values by dotted lines and the numerical values by

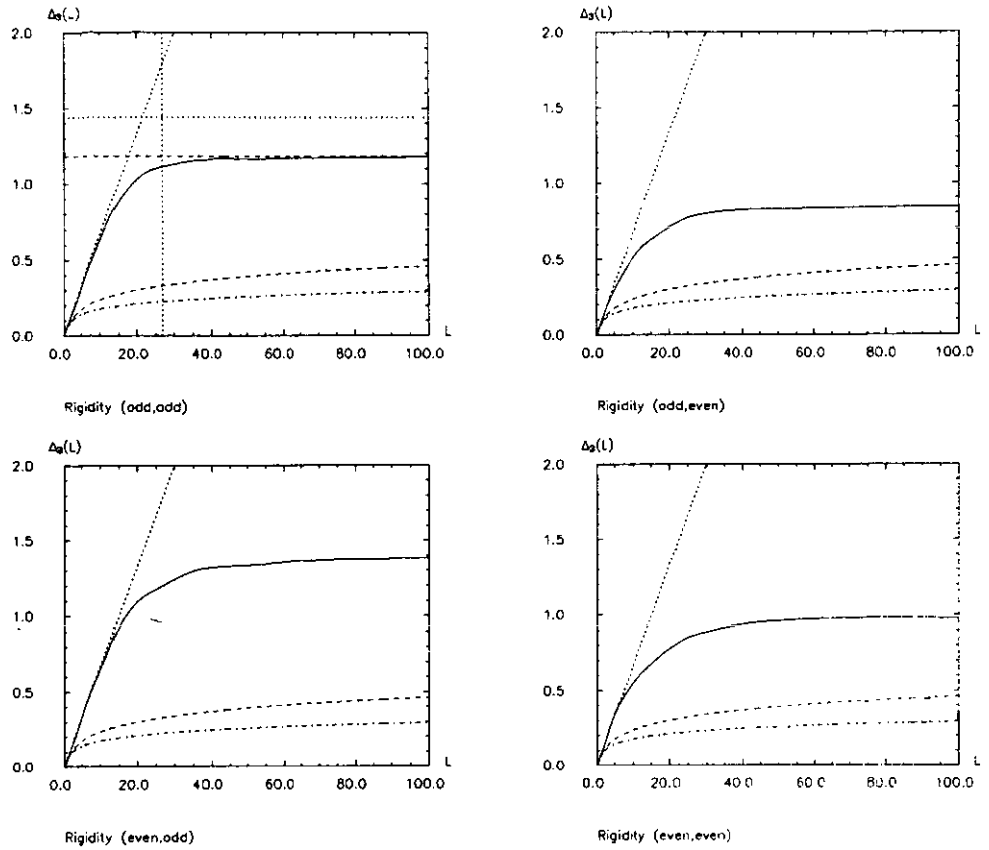

Figure 7. Rigidity $\Delta_3(L)$ for the four parity classes, i.e $E^{(-,-)}$, $E^{(-,+)}$ (top), $E^{(+,-)}$ and $E^{(+,+)}$ (bottom).

dashed lines, respectively. The theoretical crossover value $L_{\max} \simeq 27$ is clearly distinguishable, i.e. where the $L/15$-behaviour changes into the saturation value. Considering the quite rudimentary approximations the results are very reasonable. Note that only for the (odd, odd) parity class statements can be made, because this is the only pure Dirichlet–Dirichlet billiard. We also see that in the (odd, odd) case the theoretical value is too large which shows that here our approximation of two almost equal shortest geodesics along the X- and Y-axis is not very good. The fact that $\Delta_3(L)$ becomes a very slowly increasing function for $L \to \infty$ indicates that the level sequence becomes a rather regular sequence. From equation (3.1) we know that the sequence of energy levels for $E \to \infty$ is in fact a regular sequence and therefore rigid.

Of course, we can repeat our considerations for the entire square with all parity classes. Here the predictions are

$$L_{\max} \simeq 55 \qquad \Sigma_\infty^{\text{theory}} \simeq 5.84 \qquad \Delta_\infty^{\text{theory}} \simeq 2.92. \tag{3.20}$$

The numerical results are ($\Sigma_\infty^{\text{num}}$ is the mean value for $L > 20$)

$$\Sigma_\infty^{\text{num}} \simeq 6.66 \qquad \Delta_\infty^{\text{num}} \simeq 3.118 \tag{3.21}$$

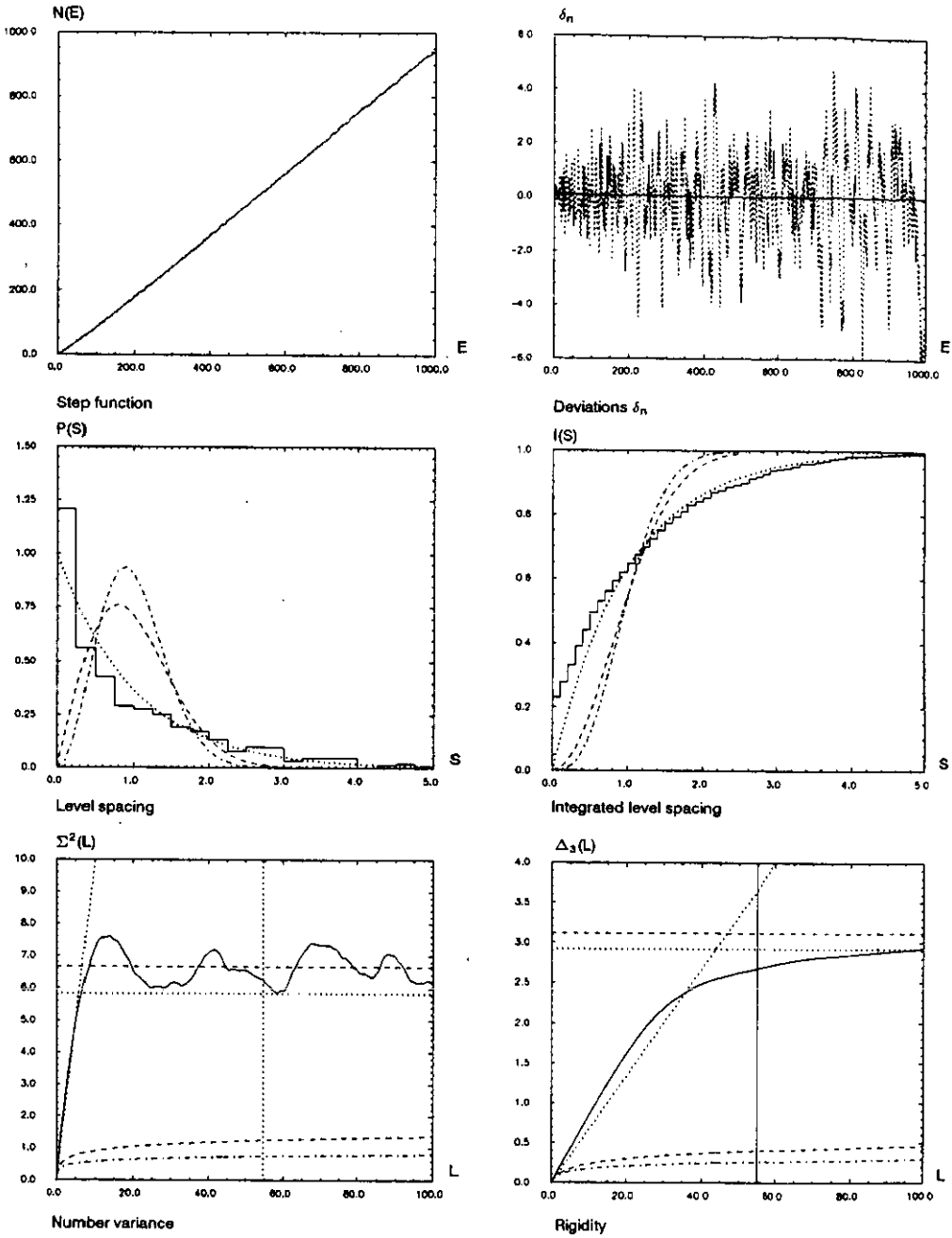

Figure 8. Analysis for the entire square.

and the fit parameters for $\Delta_\infty^{\text{num}}$ are $a = 4.650$ and $b = 170.24$, respectively. Here $\Sigma_\infty^{\text{num}} - 2\Delta_\infty^{\text{num}} \simeq 0.43$. In figure 8 I have indicated the theoretical values by dotted lines and the numerical results by dashed lines. All features are repeated. Whereas the agreement with the theoretical and numerical values for the spectral rigidity give very good results (compare the (odd, odd) case), the actual number variance lies

Table 3. The spectral rigidity and Berry's theory

N	L_{max}	Δ_∞^{theory}	Δ_{max}	$\Delta_{max}/\sqrt{\mathcal{E}}$	Δ_∞	$\Delta_\infty/\sqrt{\mathcal{E}}$
100	17.1	0.947	0.825	0.083	0.825	0.083
200	25.3	1.350	1.50	0.105	1.49	0.105
300	30.6	1.634	1.82	0.105	1.85	0.107
400	35.3	1.885	2.13	0.106	2.15	0.108
500	40.0	2.118	2.29	0.102	2.32	0.104
600	43.4	2.318	2.28	0.093	2.35	0.096
700	46.9	2.503	2.25	0.085	2.35	0.089
800	50.1	2.676	2.72	0.096	2.80	0.090
900	53.2	2.840	2.85	0.095	3.10	0.101
952	54.7	2.920	2.925	0.095	3.12	0.101

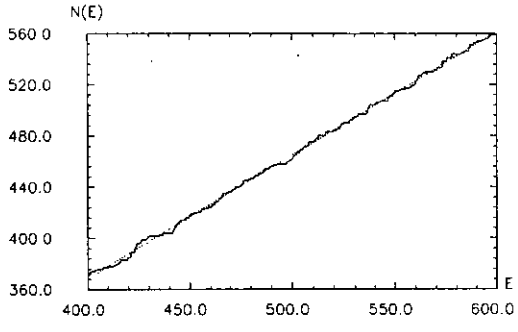

Figure 9. Detail of Weyl's law.

above the theoretical expectation.

In table 3 I have listed the comparison with the numerical results for the spectral rigidity and the theoretical predictions à la Berry for the entire square. A maximum of 952 levels have been taken into account with $E \leqslant 1000$. In the first column I have indicated the number of energy levels $N \simeq \mathcal{E}$ taken into account for the calculation of the spectral rigidity, in the second column L_{max} according to $L_{max} \simeq \sqrt{\pi\mathcal{E}}$, in the third Δ_∞ according to equation (3.16), in the forth the numerical result for the calculated maximum $\Delta_{max} = \Delta_3(100)$ of the spectral rigidity, in the fifth the resulting quotient of Δ_{max} and $\sqrt{\mathcal{E}}$, and in the sixth and seven the analogue of the former two columns for the corrected numerical Δ_∞. Our numerical results are in agreement with Berry's theory. The mean value for $\Delta_{max}/\sqrt{\mathcal{E}}$ is given by 0.097 ± 0.003, whereas for $\Delta_\infty/\sqrt{\mathcal{E}}$ by 0.099 ± 0.003, in excellent agreement with the theoretical value 0.0947. Note that Δ_∞^{num} gives somewhat larger values, which can be explained by the fact that our rectangle in the hyperbolic geometry is a distorted geometrical object with only almost equal sides ($L_0 \simeq L_1$, see above), whereas the semi-classical theory for the spectral rigidity of Berry deals with a flat square.

Figure 9 shows an enlargement of the step-function. We can clearly see the excellent agreement with the prediction of Weyl's law. Also we can see the periodic fluctuation about it, a very typical feature of separable systems.

4. Discussion and summary

In this paper I have discussed a particular quantum billiard in the hyperbolic strip in

the form of a rectangle, consisting of two vertical and two horizontal straight lines. The motivation for an investigation of this model was threefold.

(i) To study a separable quantum billiard in the hyperbolic plane.

(ii) To investigate the statistical properties of the energy levels with respect to predictions of separable systems and the semi-classical theory of Berry for the spectral rigidity.

(iii)To compare the results with a typically chaotic model (the regular octagon) in the hyperbolic geometry.

We obtained quantization conditions for the momentum (k_l fixed)

$$\text{even:} \qquad P^{ip_n}_{ik_l-1/2}(\sin Y_0) + P^{ip_n}_{ik_l-1/2}(-\sin Y_0) = 0 \tag{4.1}$$

$$\text{odd:} \qquad P^{ip_n}_{ik_l-12}(\sin Y_0) - P^{ip_n}_{ik_l-1/2}(-\sin Y_0) = 0 \tag{4.2}$$

for even and odd parity, respectively, which are transcendental equations.

For the four parity classes, with Dirichlet- and Neumann- boundary conditions, respectively, at the lines $X = 0$ and $Y = 0$, the number of levels for a given fixed energy E are $\#N^{(-,-)} < \#N^{(-,+)} \leqslant \#N^{(+,-)} < \#N^{(+,+)}$. The ground states for the four parity classes are $E_0^{(+,+)} = 2.4360$, $E_0^{(-,+)} = 4.8994$, $E_0^{(+,-)} = 5.6255$ and $E_0^{(-,-)} = 7.5219$, respectively, with $E_0^{(+,+)}$ as the lowest lying level. We have approximately $E_N^{(+,+)} < E_N^{(-,+)} \simeq E_N^{(+,-)} < E_N^{(-,-)}$ (N fixed) for all levels. These features make reasonable sense due to the general properties of quantum systems, i.e. the ground state is always an even state, etc. We also noted the proximity of the lowest lying levels of our system to the lowest lying levels of the regular octagon with periodic boundary conditions. However, the statistical properties of the energy levels of our integrable billiard systems compared with the analysis of the chaotic properties of the octagon show no relation to each other. For example, the level statistics for a generic octagon is GOE, i.e. obeying a Wigner distribution, the spectral rigidity does show saturation but the growing behaviour of Δ_∞ is different. Furthermore the regular octagon is highly symmetric, a property which gives rise to many exactly degenerate energy levels (i.e. the ground level is threefold degenerate). Nothing of these features can be found in our system and no information achieved in the integrable billiard survives in the transition to the chaotic system (compare also the results of [13, 24] with each other).

Our results were furthermore checked by Weyl's law $\bar{N}(E)$, and further statistically analysed by the level distribution $P(S)$, the integrated level distribution $I(S)$, the number variance $\Sigma^2(S)$ and spectral rigidity $\Delta_3(S)$. The level distributions $P(S)$ showed a closely Poisson-like behaviour with reasonable confidence levels for each parity class. However, the level distribution of the entire square containing all parity classes was very poorly Poisson-like with almost negligible confidence levels, in particular there are too many almost degenerated levels. Also the integrated level spacing statistics shows significant deviations. A similar effect was observed in [32] for another integrable billiard system. These rather large fluctuations of the level spacing statistics indicate that the energy level sequence is not completely random as in an uncorrelated Poisson eigenvalue sequence. Therefore the discrimination of the energy levels with respect to symmetry classes are indispensible in the statistical analysis of energy levels, a well known feature.

In the case of Dirichlet–Dirichlet boundary conditions the evaluated behaviour for the spectral rigidity (alternatively, the number variance) could be explained by

the semi-classical periodic orbit theory of Berry. We found for small values of L the universal $L/15$-behaviour and saturation for $L > L_{max}$. We found that the number variance showed precocious saturation, whereas the rigidity showed slow saturation. L_{max} and Δ_∞ could be calculated by some assumptions about the geometry of our system and theoretical and numerical results were in satisfactorily agreement. For the entire square we found $L_{max} \simeq 55$, $\Delta_\infty^{theory} \simeq 2.9197$ and $\Delta_\infty^{num} \simeq 3.118$, where Δ_∞^{num} was determined by an appropriate fit. The theoretical prediction of the spectral rigidity and the numerical results were in close agreement. It is quite satisfactory that the semi-classical theory of Berry for the spectral rigidity is applied in a straightforward and simple way.

I also discussed where the integrability comes from. Transforming the rectangle into the Poincaré upper half-plane or onto the Poincaré disc distorts it significantly and no simple treatment seems obvious, let alone integrability. However it is known that integrability and non-integrability are connected with the long-term behaviour of orbits, i.e. whether they have positive Lyapunov exponent, which depends on the focusing and defocusing behaviour of the boundaries. A genuine hyperbolic square tesselating the hyperbolic plane has geodesics as boundaries with curvature zero, however the space is negatively curved everywhere. The hyperbolic rectangle as investigated is realized in the same geometry but has only two geodesics as boundaries. The remaining two (horizontal straight) line have positive curvature, therefore effectively annihilate the chaos-creating negative curvature property of hyperbolic space. Note that the hyperbolic squares, as generated by the matrices (2.7), compare figures 1(*a–c*), tesselate the hyperbolic plane only in the case of $N\alpha = 2\pi$ with α as in equation (2.8), $N \in \mathbb{N}$, and the Riemann surface interpretation is not valid for these squares.

The model of a 'rectangular approximation' of regular or irregular octagons must be considered as not successful, and it remains doubtful whether integrable approximations are able to give information of a suitable corresponding chaotic system at all. However, the present model is a further example of a non-trivial billiard system, in particular the fact that it is a billiard in the hyperbolic plane, a space with everywhere constant negative curvature.

Acknowledgments

I would like to thank the organizers of the symposium 'Hyperbolic Spaces and Mathematical Physics' in Bielefeld (Germany), S Albeverio, H Helling, J L Mennicke and A B Venkov for their invitation and fruitful discussions. Furthermore I would like to thank M Sieber for providing useful help in the statistical analysis and R Aurich and F Steiner for a critical reading of the manuscript and useful comments. I also thank the members of the II. Institut für Theoretische Physik, Hamburg University, for their hospitality.

References

[1] Gutzwiller M C 1967 *J. Math. Phys.* **8** 1979; 1969 *J. Math. Phys.* **10** 1004; 1970 *J. Math. Phys.* **11** 1791; 1971 *J. Math. Phys.* **12** 343

[2] Friedrich H and Wintgen D 1989 *Phys. Rep.* **183** 37

[3] Sieber M 1991 The hyperbola billiard: a model for the semiclassical quantization of chaotic systems *Preprint* **DESY 91-030**, *PhD thesis*
[4] Sieber M and Steiner F 1990 *Phys. Lett.* **144A** 159; *Physica* **44D** 248; 1991 *Phys. Rev. Lett.* **67** 1941
[5] Hejhal D A 1976 *The Selberg Trace Formula for* $PSL(2, \mathbf{R})$ vol I *(Lecture Notes in Mathematics 548)* (Berlin: Springer)
[6] Selberg A 1956 *J. Indian Math. Soc.* **20** 47
[7] Berry M V 1987 *Proc. R. Soc.* A **413** 183
[8] Aurich R, Sieber M and Steiner F 1988 *Phys. Rev. Lett.* **61** 483
Aurich R, Bogomolny E B and Steiner F 1991 *Physica* **48D** 91
Aurich R and Steiner F 1991 From classical periodic orbits to the quantization of chaos *Preprint* DESY 91-044
[9] Aurich R and Steiner F 1990 *Physica* **43D** 155
[10] Aurich R and Steiner F 1991 *Phys. Rev.* A **45** 583
[11] Kac M 1966 *Am. Math. Monthly (part II)* **73** 1
[12] Graham R and Szépfalusy P 1990 *Phys. Rev.* D **42** 248
[13] Matthies C and Steiner F 1991Phys. Rev. A447877
[14] Argyres E N, Papadopoulos C G, Papadontopoulos E and Tamvakis E 1989 *J. Phys. A: Math. Gen.* **22** 3577
[15] Green M B, Schwarz J H and Witten E 1984 *Superstring Theory I and II* (Cambridge: Cambridge University Press)
[16] D'Hoker E and Phong D H 1988 *Rev. Mod. Phys.* **60** 917
[17] Polyakov A M 1981 *Phys. Lett.* B **103** 207
[18] Gutzwiller M C 1985 *Phys. Scr.* T **9** 184
[19] Steiner F 1987 *Recent Developments in Mathematical Physics (Conference Schladming 1987)* ed H Mitter and L Pittner (Berlin: Springer) p 305
[20] Bunimovich L A 1991 *Talk at symposium 'Hyperbolic Spaces and Mathematical Physics', Bielefeld (Germany), June 1991, unpublished*
[21] Donnay V J 1991 *Commun. Math. Phys.* **141** 225
[22] Balazs N L and Voros A 1986 *Phys. Rep.* **143** 109
[23] Balazs N L, Schmit C S and Voros A 1987 *J. Stat. Phys.* **46** 1067
Schmit C 1991 Quantum and classical properties of some billiards on the hyperbolic plane *Chaos and Quantum Physics (Les Houches Lectures 1989, Session LII)* ed M J Giannoni, A Voros and J Zinn-Justin (Amsterdam: North-Holland)
[24] Csordas A, Graham R and Szépfalusy P 1991 *Phys. Rev.* A **44** 1491
Graham G, Hübner R, Szépfalusy P and Vattay G 1991 *Phys. Rev.* A **44** 7002
[25] Grosche C 1990 *Fortschr. Phys.* **38** 531
[26] Weyl H 1912 *Math. Ann.* **71** 441
[27] Baltes H P and Hilf E R 1976 *Spectra of Finite Systems* (Mannheim: Bibliographisches Institut Mannheim)
[28] Stewartson K and Waechter R T 1971 *Proc. Camb. Phil. Soc.* **69** 353
[29] Baltes H P 1972 *Phys. Rev.* A **6** 2252
[30] Brownell F H 1955 *Pacific J. Math.* **5** 483; 1957 *J. Math. Mech.* **6** 119
[31] Waechter R T 1972 *Proc. Cam. Phil. Soc.* **72** 439
[32] Casati C, Chirikov B V and Guarneri I 1985 *Phys. Rev. Lett.* **54** 1350
[33] Dyson F J and Metha M L 1963 *J. Math. Phys.* **4** 701
[34] Brody T A, Flores J, French J B, Mello P A, Pandey A and Wong S S M 1981 *Rev. Mod. Phys.* **53** 385
[35] Berry M V 1985 *Proc. R. Soc.* A **400** 229
[36] Haq R U, Pandey A and Bohigas O 1982 *Phys. Rev. Lett.* **48** 1086; 1985 *Phys. Rev. Lett.* **54** 1645
[37] Lane A M 1957 *Oak Ridge National Laboratory Report ORLN-2309* unpublished
reprinted in:
Porter C E 1965 *Statistical Theories of Spectra: Fluctuations* (New York: Academic) p 212